European Journal of Medicinal Chemistry 168 (2019) 1–10

Contents lists available at ScienceDirect

European Journal of Medicinal Chemistry

journal homepage: http://www.elsevier.com/locate/ejmech

Research paper

Design, synthesis and biological evaluation of 2-(phenoxymethyl)-5-phenyl-1,3,4-oxadiazole derivatives as anti-breast cancer agents

K. Lakshmithendral [a], K. Saravanan [a], R. Elancheran [a], K. Archana [a], N. Manikandan [b], H.A. Arjun [a], M. Ramanathan [b], N.K. Lokanath [c], S. Kabilan [a, *]

[a] Drug Discovery Lab, Department of Chemistry, Annamalai University, Annamalai Nagar, 608002, Tamil Nadu, India
[b] Department of Pharmacology, PSG College of Pharmacy, Coimbatore, 641004, Tamil Nadu, India
[c] Department of Studies in Physics, University of Mysore, Manasagangotri, Mysuru, 570 006, India

ARTICLE INFO

Article history:
Received 1 December 2018
Received in revised form
9 February 2019
Accepted 10 February 2019
Available online 15 February 2019

Keywords:
Estrogen receptor
Breast cancer
1,3,4-Oxadiazoles
Molecular docking

ABSTRACT

Structural based molecular docking approach revealed the findings of 2-(phenoxymethyl) -5-phenyl-1,3,4-oxadiazole derivatives. The compounds (**7a-o**) were synthesized and characterized well by using conventional methods. The compounds, **7b** and **7m** were reconfirmed through single crystal XRD analysis. The synthesized compounds (**7a-o**) were evaluated their antiproliferative activities against MCF-7 and MDA-MB-453. Furthermore, Lipinski's rule of five and pharmacokinetic properties were predicted for the test compounds. These results demonstrate that the compounds **7b** and **7d** exhibit more potent cytotoxicity and **7d** exhibits dose-dependent activity and reduced cell viability. Further, the mechanism of action for the induced apoptosis was observed through morphological changes and western blotting analysis. These findings may furnish the lead for further development.

1. Introduction

Cancer is a group of heterogeneous diseases involving dysregulation of cell growth and functions to proliferate to other parts of the body. Breast cancer (BCa) is the second most common cancer worldwide. National Cancer Institute (NCI) has assessed that the diagnosis of 266,120 new cases and 40,920 dying due to BCa in the United States in 2018 [1,2]. The global burden of BCa surpasses all other cancers, and the frequency is still rising. Over the last decade, several drugs and monoclonal antibodies have been approved and are in the advanced stages of clinical trials that target the receptors and signaling pathways [3]. ER-positive (ER+) breast cancer is estrogen-dependent including luminal types A and B. ER-negative (ER-) breast cancer is estrogen independent including the subtypes human epidermal growth factor receptor 2 (HER2) in which ErbB2 is overexpressed [3]. Tamoxifen is a non-steroidal antiestrogen and widely used for the treatment of breast cancer, which acts on estrogen receptor [4]. Inhibition of cancerous inhibitor of protein phosphatase 2A (CIP2A) determines the effects of tamoxifen-induced apoptosis in ER-negative breast cancer cells [5]. ER alpha, ER beta, and Progesterone receptor are not expressed in Triple-negative breast cancer (TNBC) which still exhibits an extraordinary clinical challenge due to the unavoidably ineluctable advancement of medical obstruction [6]. DNMT3B (DNA Methyltransferase 3 Beta) is a Protein-Coding gene, which is related to abnormal methylation of tumour suppressor and repair genes and its overexpression contributes to oncogenic processes and tumorigenesis [7]. OTUD1 (ovarian tumour deubiquitinase 1) represses breast cancer metastasis by mitigating Transforming growth factor beta (TGF-β) induced pro-oncogenic responses via deubiquitination of SMAD7 (SMAD Family Member 7) which is a protein-coding gene [8]. The five-membered heterocyclic compound containing more than two heteroatoms like azole, thiazole, oxadiazole, triazene, imidazole, purines, etc. have tremendous importance in human life due to their assortment of medicinal applications against several maladies [9,10].

In recent years, the structural activity relationship with target structures and their mechanism used for the drug design and oxadiazole has been reported with various biological activities such as antitubercular, antiviral, antifungal, antibacterial, antimicrobial, antidiabetic and anticancer activities [11–14]. In particular, 1,3,4-oxadiazole is an important moiety that exhibits more potent and selective inhibitory activity against various cancer cell lines.

* Corresponding author. Drug Discovery Lab, Department of Chemistry, Annamalai University, Annamalai Nagar, 608002, Tamil Nadu, India.
E-mail address: profdrskabilanau@gmail.com (S. Kabilan).

https://doi.org/10.1016/j.ejmech.2019.02.033
0223-5234/

Compound **1** with p-methoxybenzenesulfonamido moiety showed more than 80% mean percentage inhibition at 10 μM concentration against breast cancer cell line, MDA-MB-468 [15]. Compound **2** exerted submicromolar IC_{50} values of 0.67, 0.80, and 0.87 μM against prostate cancer cell line (PC-3), colon cancer cell line (HCT-116), and kidney adenocarcinoma cell line (ACHN) respectively. Also, it exhibited anti-proliferative potential against MDA-MB-231 breast cancer cell line [16,17]. MCF-7 is a breast cancer cell line which retained several characteristics of differentiated mammary epithelium, including the ability to process estradiol via cytoplasmic estrogen receptors and the capability of forming domes [18]. Organotin compounds showed higher activity against breast cancer cells MCF-7 (ER-positive) than against MDA-MB-231 (ER-negative) indicating that estrogen receptors may also be involved in their antitumour mechanism [19,20]. A novel silver iodide metalodrug exhibits equal activity against MDA-MB-231 cells where estrogen receptors (ERs) are devoid with the one against MCF-7 where ERs are present [21]. MDA-MB-453 is human breast cancer cell line that has an active glycerol 3-phosphate shuttle and expresses high amounts of functional androgen receptor [22]. Nimesulide, Aspirin and salicylic acid metal complexes have high binding affinity against DNA and their stronger inhibitory activity against Lipooxygenase (LOX) [23,24]. Taken together, the 1,3,4-oxadiazole derivatives were designed and depicted in Fig. 1. Herein, we reported the design, synthesis and biological evaluation of a series of novel 2-(phenoxymethyl)-5-phenyl-1,3,4-oxadiazole derivatives.

2. Results and discussion

2.1. Molecular modeling

Molecular docking approach is followed for the designing of 1,3,4-oxadiazole derivatives by using the Schrödinger (Maestro 11.2) software [25]. The structure of human estrogen receptor alpha ligand-binding domain in complex with 4-hydroxytamoxifen (PDB ID: 3ERT, resolution 1.9 Å) was obtained from the protein data bank, refined the raw structure and utilized for this study [26]. We have found that the compounds (**7a-o**) depicted specific van der Waals (vdW) interactions with the surrounding hydrophobic residues LEU 346, ALA 350, LEU 384, LEU 387, MET 388, LEU 391, ILE 424 and form hydrogen bonds through the cyano group with two residues (GLU 353, and ARG 394) in the Helix 12. Of these, the best scoring pose of the compounds (**7b & 7d**) from the docking studies is shown in Fig. (2) along with receptor residues which interact with the ligands within binding sites.

From the docking studies, we found that the compounds, **7b & 7d** showed the highest Glide score (−9.968 and −9.982 kcal/mol respectively). The compounds (**7a-o**) have shown binding affinity to ER, and their docking scores were related to the standards (Table 1). The compounds (**7b, 7d, 7g-k)** has highest binding energy in the range of −9.1 to −9.9 kcal/mol and the glide energy vary from −46.364 to −35.322 kcal/mol. The standards, Imatinib and Tamoxifen glide energy were −55.298 and −57.000 kcal/mol respectively. These studies were well established, and the results were concertized with our previously reported work [34–38].

2.2. Chemistry

Molecular docking results intend the synthesis of the compounds (**7a-o**). The compounds (**6a-e**) were synthesized from the commercially available benzoic acid by esterification, hydrazine hydrate then refluxed with chloroacetic acid and $POCl_3$ [27,28]. Further, the compounds (**7a-o**) were obtained by the reaction of the compounds (**6a-e**) with substituted phenol in the presence of K_2CO_3 and KI in DMF for 1–2 h, in moderate to excellent yield, 70–90%. The general synthesis of 2-(phenoxymethyl)-5-phenyl-1,3,4-oxadiazole derivatives (**7a-o**) is depicted in Scheme 1.

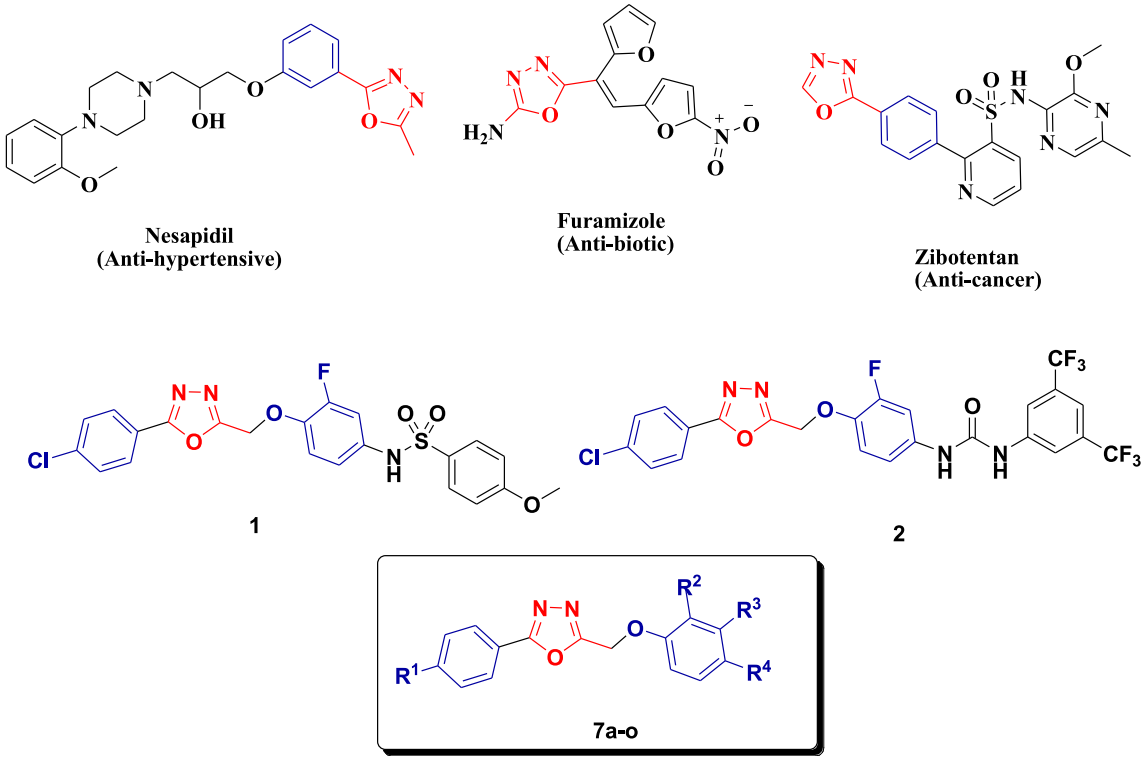

Fig. 1. Structural modification of designed oxadiazole derivatives.

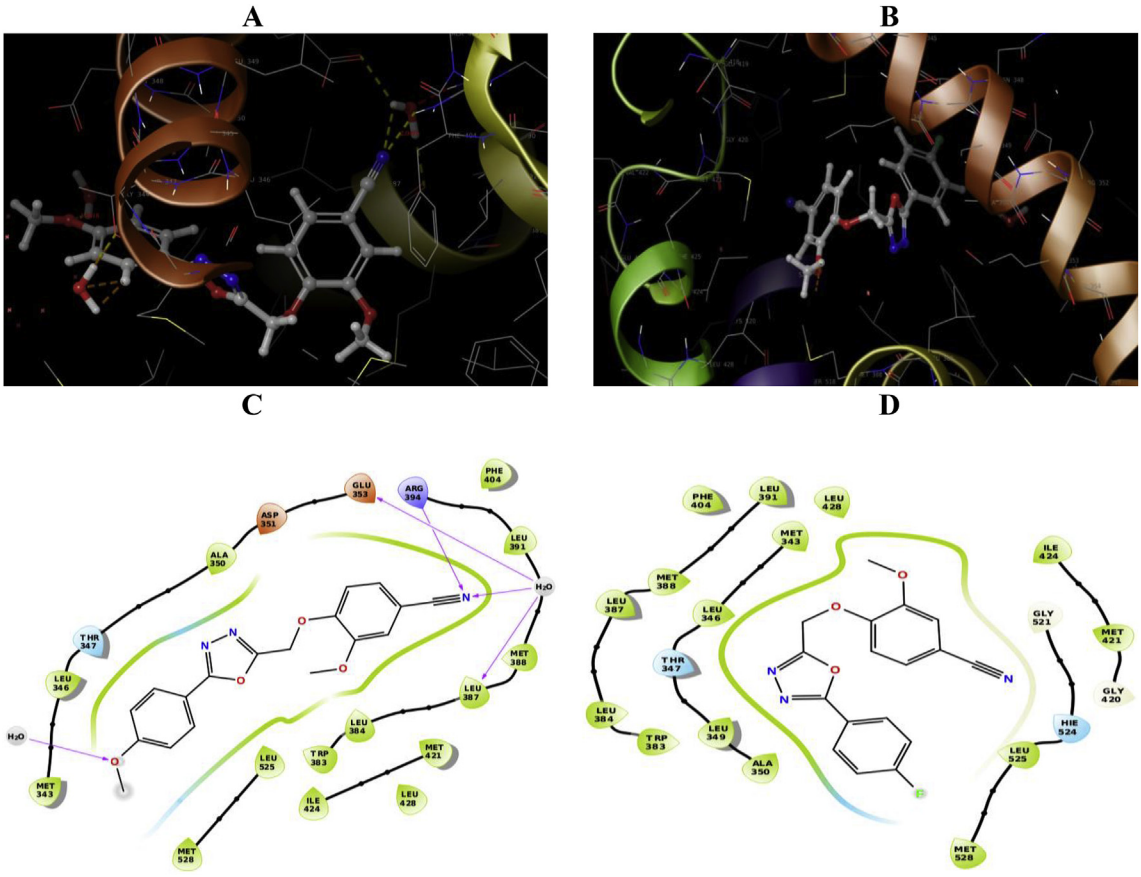

Fig. 2. Predicted binding mode of the compounds (**7b** & **7d**) in ER LBD (PDB: 3ERT) highlighting the H-Bond and specific hydrophobic interactions (Fig. 2A and B: coloured by atom types- C light gray, F green, N blue, O red, H white). (For interpretation of the references to colour in this figure legend, the reader is referred to the Web version of this article.)

Table 1
Lowest binding energy for the compounds in the ER (PDB ID: 3ERT).

Compound	glide gscore	glide evdw	glide ecoul	glide energy	Interacting Residues (3ERT)
7a	−6.944	−35.772	−0.115	−35.887	–
7b	−9.968	−35.748	−3.738	−39.486	ARG 394, GLU 353, LEU 387, HOH
7c	−7.401	−33.415	−3.753	−37.168	ARG 394
7d	−9.982	−36.18	0.857	−35.322	–
7e	−6.982	−37.661	−3.604	−41.265	CYS 530, HOH
7f	−8.531	−40.919	−0.014	−40.933	–
7g	−9.222	−37.286	−2.413	−39.699	ARG 394, HOH
7h	−9.72	−42.32	0.009	−42.311	–
7i	−9.353	−34.073	−2.701	−36.774	ARG 394, LEU 387, GLU 353, HOH
7j	−9.466	−36.448	−2.75	−39.198	ARG 394, LEU 387, GLU 353, HOH
7k	−9.171	−42.126	0.892	−41.234	–
7l	−8.29	−36.226	−4.354	−40.58	ARG 394, GLU 353, LEU 387, HOH
7m	−7.724	−38.491	0.204	−38.287	–
7n	−8.044	−36.715	−2.809	−39.524	ARG 394, GLU 353, LEU 387, HOH
7o	−8.325	−42.907	−3.457	−46.364	ARG 394, GLU 353, LEU 387, HOH
Imatinib	−9.178	−51.793	−3.505	−55.298	–
Tamoxifen	−13.042	−50,841	−6.158	−57.000	H- Bond interaction with HOH

glide evdw = van der Waals interaction energies, glide ecoul = Coulomb interaction energies.

The synthesized compounds (**7a-o**) were well characterized by IR, NMR, and HRMS, and all the data are in accordance with the proposed structures. Single crystals of the compounds, **7b** and **7m** were obtained from ethyl acetate/petroleum ether solvent by slow evaporation at room temperature [29]. The compound, **7b** belongs to triclinic system with space group, P-1, a = 6.0847 (14) Å, b = 8.5048 (19) Å, c = 17.286 (4) Å, $\alpha = 102.668°$ (7), $\beta = 90.646°$ (6), $\gamma = 109.813°$ (8) and Z = 2 [30]. Similarly, the compound, **7m** belongs to triclinic system with space group, P-1, a = 8.45 (6) Å, b = 10.79 (8) Å, c = 11.03 (8) Å, $\alpha = 113.63°$ (4), $\beta = 96.51°$ (2), $\gamma = 111.65°$ (8) and Z = 2. The ORTEP structure of the compounds, **7b** and **7m** were illustrated in Fig. 3 (Table S2).

In compound **7b**, the 4-methoxyphenyl and oxadiazole (r.m.s. deviation 0.007 Å) rings are almost coplanar with a dihedral angle of 1.4. The methoxy atoms O4 and C16 are also coplanar with the rings, deviating by 0.080 and 0.020 Å from the mean plane of the

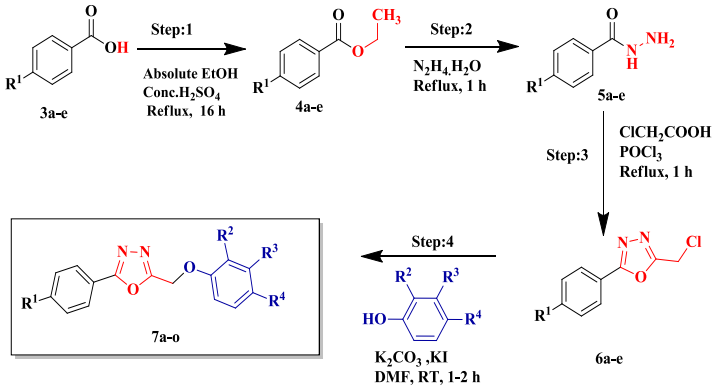

ID	R^1	R^2	R^3	R^4
7a	H	OCH_3	H	H
7b	**OCH_3**	**OCH_3**	**H**	**H**
7c	CH_3	OCH_3	H	H
7d	**F**	**OCH_3**	**H**	**H**
7e	Cl	OCH_3	H	H
7f	H	H	F	H
7g	OCH_3	H	F	H
7h	CH_3	H	F	H

ID	R^1	R^2	R^3	R^4
7i	F	H	F	H
7j	Cl	H	F	H
7k	H	H	H	
7l	OCH_3	H	H	
7m	CH_3	H	H	
7n	F	H	H	
7o	Cl	H	H	

Scheme 1. Synthesis of oxadiazole derivatives.

phenyl ring, respectively. The compound **7b** is associated via C—H···O interactions into inversion dimers (C16—H16B···O3). In addition, offset π–π interactions are observed between the centroids of inversion-related oxadiazole and 4-methoxyphenyl rings with a centroid-centroid distance of 3.700 Å and slippage of 1.037 Å. Similarly, in compound **7m,** the methyl phenyl ring is almost coplanar with the oxadiazole ring, the angle between their mean planes being 4.0 and is associated via C—H···O interactions. Also, offset π–π interactions are observed between the centroids of inversion-related oxadiazole and methyl phenyl rings with a centroid-centroid distance of 3.720 Å, and the shift distance is 1.078. The distance between C2 and O3 is 15.660.

2.3. Biological evaluation

All the synthesized compounds (**7a-o**) were evaluated for the anticancer activities against breast cancer cell lines (MCF-7 & MDA-MB-453) and their cytotoxicity using non-cancerous cell line (MCF-10A) as compared with the standard, Imitanib by using MTT assay. Cytotoxicity assays assess the integrity of the cell's plasma membrane, and it was determined in the presence and absence of the compounds as described in the earlier methods [31,32]. The results demonstrated that the compounds (**7a-o**) were shown the significant cytotoxic potential in MDA-MB-453 and MCF-7 cell lines in the IC_{50} range of 10–50 μM as compared with imatinib (IC_{50} 12.84 ± 2.2, 6.33 ± 1.9 respectively) (Table 2). The compounds, **7b** and **7d,** showed the highest activities against MCF-7 cell lines (IC_{50} 12.95 ± 3.3 and 10.51 ± 1.9 respectively) and MDA-MB-453 (IC_{50} 11.12 ± 2.1 and 10.25 ± 2.5 respectively). It suggested that the CN group at R^4 and methoxy group at R^2 has influenced the anticancer activities. Also, the replace of H to F atom at R^3 has slightly decreased the IC_{50} values. Similarly, at R [4], CN group has better activities that 1,3,4-oxadiazole group. This comparison was beneficial for improving the efficacy of the compounds. Also, the compounds, **7b** and **7d** have not shown the toxicity against MCF-10A which reliably represent normal human mammary cells.

From these series, the compounds, **7b** and **7d** showed the promising anti-breast cancer activities in MDA-MB-453 and MCF-7 cell lines. It is manifest that the groups especially OCH_3, F in the R^1 and R^2 substitutions were determining the anticancer activities in the cell proliferation assays. The compound, **7d** exhibits dose-dependent activity in triple negative breast cancer cell lines. The IC_{50} value was calculated as ~10 μM for this active compound shown in Fig. 4. The compound, **7d** reduced cell viability and induced the apoptosis confirmed through AO/EtBr staining [33].

The western blotting analysis was carried out as described earlier shown in Fig. 5 [34–36]. The compound, **7d** shows DNMT 3B enzyme inhibitory activity (approx. 33%) at 100 μM concentration. Also, it exhibits only 10% activity in inhibiting the DNMT1 enzyme. Since it is more specific towards the DNMT 3B, it can be used DNMT 3B isoform targeted therapies to treat breast cancer. Dose-Dependent expression of the p53 gene was found in the

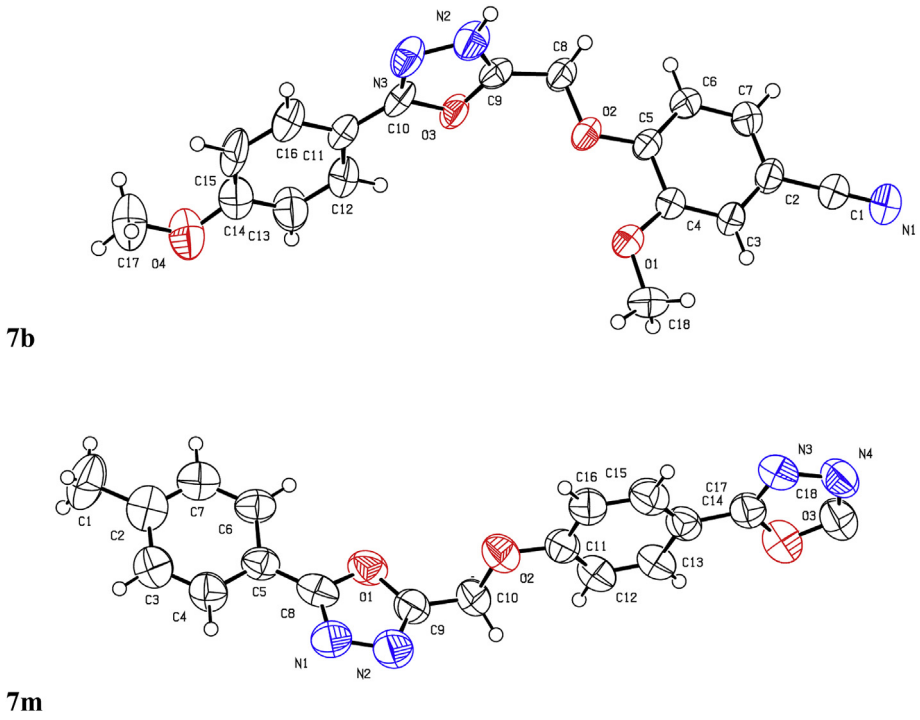

Fig. 3. ORTEP diagram of 7b & 7m.

Table 2
IC_{50} of test and standard compounds.

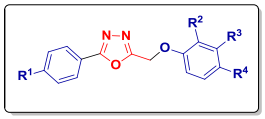

ID	R^1	R^2	R^3	R^4	MCF-7 (μM)[a]	MDA-MB-453 (μM)[a]	MCF-10A (μM)[a]
7a	H	OCH_3	H	CN	32.17 ± 2.7	40.15 ± 1.9	>100
7b	**OCH_3**	**OCH_3**	**H**	**CN**	**11.12 ± 2.1**	**12.95 ± 3.3**	**>100**
7c	CH_3	OCH_3	H	CN	27.13 ± 3.1	38.41 ± 2.7	>100
7d	**F**	**OCH_3**	**H**	**CN**	**10.25 ± 2.5**	**10.51 ± 1.9**	**>100**
7e	Cl	OCH_3	H	CN	21.54 ± 1.9	33.87 ± 1.1	89.5 ± 2.1
7f	H	H	F	CN	>50	>50	>100
7g	OCH_3	H	F	CN	42.15 ± 1.8	45.49 ± 2.9	>100
7h	CH_3	H	F	CN	>50	>50	>100
7i	F	H	F	CN	20.45 ± 0.9	25.13 ± 3.1	84.2 ± 3.2
7j	Cl	H	F	CN	48.32 ± 2.3	>50	>100
7k	H	H	H		>50	>50	>100
7l	OCH_3	H	H		31.16 ± 2.7	36.18 ± 1.1	>100
7m	CH_3	H	H		>50	>50	>100
7n	F	H	H		35.62 ± 3.2	38.19 ± 2.5	>100
7o	Cl	H	H		45.23 ± 3.1	>50	>100
Imitanib[b]					6.33 ± 1.9	12.84 ± 2.2	>100

[a] The values are the mean ± standard deviation (SD) of three independent experiments performed in triplicate.
[b] Positive control.

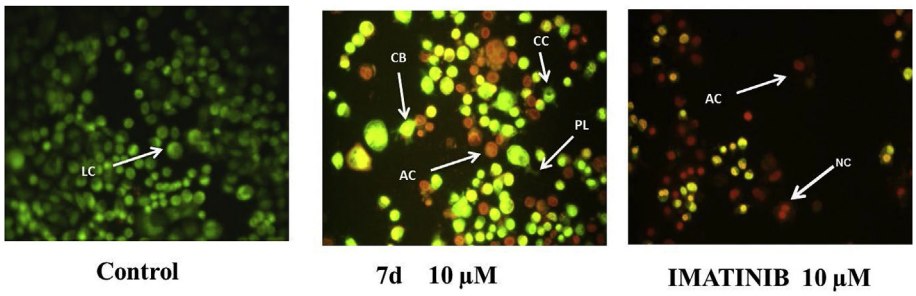

Fig. 4. Morphological changes in **7d** and imatinib treated breast cancer cell lines. The treated and untreated cells were stained with Acridine orange and Ethidium bromide and observed under an inverted fluorescent microscope. Live cells appear green, late apoptotic cells are appearing orange in colour, and necrotic cells are coloured red. Abbreviations: LC - Live Cells, CB - Cell membrane Blebbing, AC- Apoptotic Cells, NC-Necrotic Cells, PL - Protrusion elongation, CC- Chromatin Condensation. (For interpretation of the references to colour in this figure legend, the reader is referred to the Web version of this article.)

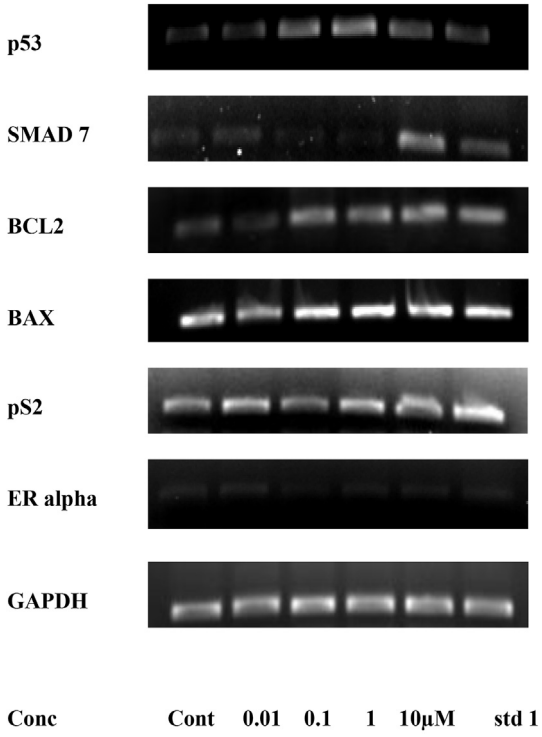

Fig. 5. Mechanism of action of the compound, **7d** which causes p53 dependent apoptotic cell death in breast cancer cells. Protein expression of SMAD7, Bcl2, Bax, pS2, and p53 was determined by western blot. GAPDH was used as loading control.

compound **7d** incubated cancer cells. It was observed that DNA double-strand repair was retained with the low level of p53 in MDA-MB-453 cell line [37]. So this compound may exhibit its beneficial effect at the dose of 0.1 μM. High dose of **7d** (10 μM) increases the SMAD7 expression in the MDA-MB-453 cell line.

The absorption, distribution, metabolism, and elimination (ADME) properties of the synthesized compounds (**7a-o**) were evaluated for the pharmacokinetic and pharmaceutical relevant properties as described earlier [35,36]. The qikpro v3.5 was used for the evaluation of ADME parameters [38], and its permissible ranges are listed in the supporting information (Table S1). In this study, the test compounds expressed the recommended drug-like properties from Lipinski's rule of five indicating zero violation and providing orally active. There were no more than 5 hydrogen bond donors and no more than 10 hydrogen bond acceptors. The molecular masses were less than 500 Da (within 290–360 ranges) and octanol-water partition coefficient was not greater than 5. In terms of Jorgensen's rules, the blockage of HERG K+ channels (−6.2 to −6.9), Caco-2 cell permeability (580–725 nm/s), the logarithm of predicted binding constant to human serum albumin (−1.5 to 1.2) were observed within the range of 95% of known drugs. There was no pharmacokinetic violation for these molecules. Overall, the pharmacokinetic results are good agreement with our previous reports [32,36].

3. Conclusion

In conclusion, the molecular docking approach was used for the designing of molecules with the estrogen receptor. The compounds, **7a-o** were synthesized and demonstrated significant anti-breast cancer activities. In particular, the compound, **7b** & **7d** were shown as the most anticipating among the series against MCF-7 and MDA-MB-453 cell lines. Also, the compounds, **7a-o** were screened in MCF-10A cell line for the toxicity. Moreover, the compound **7d** showed that it could reduce cell viability and induce apoptosis. Further, the investigation of the target site and the *in vivo* anticancer activity of the active compounds will be further examined.

4. Experimental section

4.1. Molecular modeling

The ligands for docking studies were prepared using LigPrep, Schrödinger. The ligands were geometrically refined and assigned appropriate protonation state at pH 7.0 ± 2.0. The energy minimization was carried out by OPLS 2005 force field. The protein was prepared using the protein preparation wizard in Maestro. The preprocessed protein was then used to generate a grid for docking studies. The grid was assigned by picking the ligand as the center of the grid and then the grid box was generated by applying default parameters. The docking was carried out using GLIDE, Schrödinger. GLIDE XP (extra precision) method was followed for docking calculations.

4.2. Chemistry

4.2.1. General

The entire chemicals, reagents, and solvents were procured from mercantile companies like Spectrochem, Merck, Alfa Aesar and Sigma-Aldrich, etc. The complete reactions were monitored by thin layer chromatography (TLC) via precoated aluminum plates of Merck silica gel 60 F254 furthermore visualized in UV light chamber. Column chromatography was accomplished on Merck silica gel (100–200 mesh) for the purification of intermediates. Melting points were determined by the open capillary method and are

uncorrected. Potassium bromide disk (KBr) was formulated for IR spectra attainment in the range of 4000–400 cm^{-1}. IR spectra were recorded on Thermo Nicolet FT-IR model iS5 spectrophotometer. NMR spectra attainment was done using Bruker 400 MHz AMX (^1H NMR) and 100 MHz (^{13}C NMR) in $CDCl_3$. The spectra were recorded in δ (ppm) with tetramethylsilane (TMS) as an internal standard. HRMS spectra were recorded in Thermo Exactive Orbitrap ESI-MS/MS.

*4.2.2. General procedure for preparation of substituted aromatic esters **(4a-4e)***

To a solution of substituted aromatic benzoic acid (**3a-3e**) (1 mmol) in EtOH (15 ml), a catalytic amount of Conc. H_2SO_4 was added slowly at RT, then heated to reflux for 16 h with stirring. After cooling, EtOH was removed and concentrated in *vacuum*; the reaction mixture was diluted with ethyl acetate (30 mL) and washed with sat.$NaHCO_3$ and cold water, followed by separating the organic layer. The combined organic layer was washed with brine, dried over anhydrous Na_2SO_4, filtered, concentrated, and dried under vacuum for 12 h.

*4.2.3. General procedure for preparation of aromatic acid hydrazides **(5a-5e)***

Substituted aromatic ester (1 mmol) was heated to reflux with hydrazine hydrate (2 mL) for 1 h. Upon completion of the reaction, the reaction mixture was quenched with water and extracted with ethyl acetate. The combined organic layer was washed with brine solution, dried over anhydrous sodium sulphate, filtered and concentrated under reduced pressure.

*4.2.4. General procedure for preparation of 2-(chloromethyl)-5-aryl-1,3,4-oxadiazole derivatives **(6a-6e)***

Substituted aromatic acid hydrazides (1 mmol) were heated to reflux with chloroacetic acid and phosphorus oxychloride for 1h. After completion, the reaction mixture was cooled to RT, and about 40 mL of water was added. The mixture was involved sonication for 30–40 min. The solid product was collected by filtration and dried under vacuum. The crude was purified by silica gel (100–200 mesh) column chromatography using 10–20% ethyl acetate-petroleum ether.

4.2.5. General procedure for preparation of substituted ethyl 4-hydroxybenzoate

To a solution of 4-hydroxybenzoic acid (1 mmol) in EtOH (15 ml), catalytic amount of Conc. H_2SO_4 was added slowly at RT. It had been then heated to reflux for 16 h with stirring. After cooling, removal of the EtOH and concentrated in *vacuum*, the reaction mixture was diluted with ethyl acetate (30 mL) and washed with sat.$NaHCO_3$ and cold water, followed by separating the organic layer. The combined organic layer was washed with brine, dried over anhydrous Na_2SO_4, filtered, concentrated, and dried under vacuum for 12 h.

4.2.6. General procedure for preparation of 4-hydroxybenzohydrazide

Ethyl 4-hydroxybenzoate (1 mmol) was heated to reflux with hydrazine hydrate (2 mL) for 2–3 h. The solid was washed with water and dried under vacuum for 12 h. The corresponding aromatic acid hydrazides were used without further purification.

4.2.7. General procedure for preparation of 4-(1,3,4-oxadiazol-2-yl) phenol

4-hydroxybenzohydrazide (1 mmol) was heated to reflux with triethylorthoformate (6 mL) for 16 h. After removal of the triethylorthoformate and concentrated *in vacuum*, then solid was dried under vacuum. The pale yellow solid was used without further purification.

*4.2.8. General procedure for preparation of 2-(phenoxymethyl)-5-phenyl-1,3,4-oxadiazole derivatives **(7a-7o)***

To a stirred solution of substituted phenol (1 mmol) in DMF (4 mL), K_2CO_3 (3 mmol) was added. Furthermore 2-(chloromethyl)-5-aryl-1,3,4-oxadiazole derivatives (**6a-6e**) and KI (0.5 mmol) was added. The reaction mixture was stirred at RT for 1–2 h. After completion of the reaction, the reaction mixture was washed with cold water. The solid product was collected by filtration and dried under the vacuum. It had been further crystallized in ethyl acetate/petroleum ether.

*4.2.9. 3-Methoxy-4-((5-phenyl-1,3,4-oxadiazol-2-yl)methoxy) benzonitrile **(7a)***

Yield:89%; mp: 234–236 °C, white powder; IR (KBr) ν max: 3005, 2940, 2843, 2221, 1599 cm^{-1}; ^1H NMR ($CDCl_3$, 400 MHz, ppm): δ 7.98 (d, $J = 1.6$ Hz, 2H), 7.50–7.45 (m, 3H), 7.21–7.19 (m, 2H), 7.06 (d, $J = 1.6$ Hz, 1H), 4.72 (s, 2H), 3.84 (s, 3H); ^{13}C NMR (100 MHz, $CDCl_3$, ppm): δ 166.1, 161.4, 150.5, 149.9, 132.2, 129.1, 127.1, 126.1, 123.2, 118.7, 114.9, 114.6, 106.2, 60.9, 56.2; HRMS (ESI): *m/z* calculated for $C_{17}H_{13}N_3O_3$ $[M+H]^+$ 308.10297; Found: 308.10269.

*4.2.10. 3-Methoxy-4-((5-(4-methoxyphenyl)-1,3,4-oxadiazol-2-yl) methoxy)benzonitrile **(7b)***

Yield: 92%; mp: 174–176 °C, white powder; IR (KBr) ν max: 3005, 2942, 2837, 2220, 1613, 837 cm^{-1}; ^1H NMR ($CDCl_3$, 400 MHz, ppm): δ 7.90 (d, $J = 8.4$ Hz, 2H), 7.19 (d, $J = 7.6$ Hz, 1H), 7.11 (d, $J = 8$ Hz, 1H), 7.04 (s, 1H), 6.92 (d, $J = 8$ Hz, 2H), 5.34 (s, 2H), 3.81 (d, $J = 11.2$ Hz, 6H); ^{13}C NMR (100 MHz, $CDCl_3$, ppm): δ 164.9, 161.6, 159.8, 149.5, 148.8, 127.8, 125.1, 125.0, 117.7, 114.6, 113.7, 113.5, 105.0, 59.7, 55.1, 54.4; HRMS (ESI): *m/z* calculated for $C_{18}H_{15}N_3O_4$ $[M+H]^+$ 338.11353; Found: 338.11273.

*4.2.11. 3-Methoxy-4-((5-(p-tolyl)-1,3,4-oxadiazol-2-yl)methoxy) benzonitrile **(7c)***

Yield: 87%; mp: 172–174 °C, white powder; IR (KBr) ν max: 3003, 2936, 2843, 2219, 1601, 847 cm^{-1};^1H NMR ($CDCl_3$, 400 MHz, ppm): δ 7.87 (d, $J = 7.6$ Hz, 2H), 7.25–7.21 (m, 3H), 7.11–7.05 (m, 2H),5.36 (s, 2H), 3.83 (s, 3H), 2.35 (s, 3H); ^{13}C NMR (100 MHz, $CDCl_3$, ppm): δ 166.2, 161.2, 150.6, 149.9, 142.9, 129.8, 127.1, 126.2, 120.5, 118.7, 114.9, 114.6, 106.2, 61.01, 56.2, 21.7.; HRMS (ESI): *m/z* calculated for $C_{18}H_{15}N_3O_3$ $[M+H]^+$ 322.11862; Found: 322.11954.

*4.2.12. 4-((5-(4-fluorophenyl)-1,3,4-oxadiazol-2-yl)methoxy)-3-methoxybenzonitrile **(7d)***

Yield: 98%; mp: 162–164 °C, white powder; IR (KBr) ν max: 2934, 2221, 1601, 1022, 845 cm^{-1}; ^1H NMR ($CDCl_3$, 400 MHz, ppm): δ 7.99–8.02 (m, 2H), 7.23–7.6 (m, 5H), 5.37 (s, 2H), 3.84 (s, 3H); ^{13}C NMR (100 MHz, $CDCl_3$, ppm): δ 164.2, 164.0 (d, $J = 253$ Hz), 160.4, 149.4, 148.8, 128.5 (d, $J = 9$ Hz), 125.1, 118.5, 117.6, 115.5 (d, $J = 22$ Hz), 113.8, 113.4, 105.2, 59.7, 55.1; HRMS (ESI): *m/z* calculated for $C_{17}H_{12}FN_3O_3$ $[M+H]^+$ 326.09355; Found: 326.09698.

*4.2.13. 4-((5-(4-chlorophenyl)-1,3,4-oxadiazol-2-yl)methoxy)-3-methoxybenzonitrile **(7e)***

Yield: 83%; mp: 164–166 °C, white powder; IR (KBr) ν max: 3086, 2999, 2938, 2221, 1599, 847, 730 cm^{-1}; ^1H NMR ($CDCl_3$, 400 MHz, ppm): δ 7.93 (d, $J = 8.4$ Hz, 2H), 7.43 (d, $J = 8.8$ Hz, 2H), 7.2–7.19 (m, 1H), 7.11–7.06 (m, 2H), 5.37 (s, 2H), 3.84 (s, 3H); ^{13}C NMR (100 MHz, $CDCl_3$, ppm): δ 164.2, 160.5, 149.5, 148.8, 137.6, 128.5, 127.4, 125.1, 120.7, 117.6, 113.8, 113.5, 105.3, 59.8, 55.2; HRMS (ESI): *m/z* calculated for $C_{17}H_{12}ClN_3O_3$ $[M+H]^+$: 342.06400; Found:

342.06351.

*4.2.14. 2-Fluoro-4-((5-phenyl-1,3,4-oxadiazol-2-yl)methoxy) benzonitrile **(7f)***

Yield: 82%; mp: 148–150 °C, white powder; IR (KBr) ν max: 3108, 2928, 2231, 1619, 1122 cm^{-1}; ^1H NMR ($CDCl_3$, 400 MHz, ppm): δ 7.99 (d, *J* = 7.2, 2H), 7.53–7.43 (m, 4H), 6.89–6.84 (m, 2H), 5.32 (s, 2H); ^{13}C NMR (100 MHz, $CDCl_3$, ppm): δ 165.1, 163.4 (d, *J* = 257 Hz), 161.2, 161.1, 159.7, 133.64, 133.62, 131.3, 128.1, 126.1, 122.0, 112.8, 110.6, 110.5, 102.7, 102.5, 93.9, 93.7, 59.1; HRMS (ESI): *m/z* calculated for $C_{16}H_{10}FN_3O_2$ $[M+H]^+$: 296.08298; Found: 296.08612.

*4.2.15. 2-Fluoro-4-((5-(4-methoxyphenyl)-1,3,4-oxadiazol-2-yl) methoxy)benzonitrile **(7g)***

Yield: 92%; mp: 150–152 °C, white powder; IR (KBr) ν max: 3090, 2936, 2845, 2231, 1619, 1029, 870 cm^{-1}; ^1H NMR ($CDCl_3$, 400 MHz, ppm): δ 7.92 (d, *J* = 8.8 Hz, 2H), 7.50–7.48 (m, 1H), 6.935 (d, *J* = 8.8 Hz, 2H), 6.87–6.83 (m, 2H), 5.29 (s, 2H), 3.81 (s, 3H); ^{13}C NMR (100 MHz, $CDCl_3$, ppm): δ 165.0, 163.4 (d, *J* = 258 Hz), 161.7, 161.3, 161.2, 159.2, 133.6, 133.5, 127.9, 114.4, 113.5, 112.9, 110.6, 110.5, 102.7, 102.4, 93.8, 93.6, 59.1, 58.9, 54.4; HRMS (ESI): *m/z* calculated for $C_{17}H_{12}FN_3O_3$ $[M+H]^+$: 326.09335; Found: 326.09695.

*4.2.16. 2-Fluoro-4-((5-(p-tolyl)-1,3,4-oxadiazol-2-yl)methoxy) benzonitrile **(7h)***

Yield: 85%; mp: 132–134 °C, white powder; IR (KBr) ν max: 3106, 2879, 2229, 1616, 1017, 813 cm^{-1}; ^1H NMR ($CDCl_3$, 400 MHz, ppm): δ 7.87 (d, *J* = 7.6 Hz, 2H), 7.52–7.49 (m, 1H), 7.24 (d, *J* = 7.6 Hz, 2H), 6.89–6.83 (m, 2H), 5.30 (s, 2H), 2.36 (s, 3H); ^{13}C NMR (100 MHz, $CDCl_3$, ppm): δ 166.3, 164.4 (d, *J* = 258 Hz), 162.3, 162.2, 160.5, 143.1, 134.6, 129.9, 127.1, 120.3, 113.8, 111.65, 111.62, 103.8, 103.5, 95.0, 94.8, 60.3, 21.7; HRMS (ESI): *m/z* calculated for $C_{17}H_{12}FN_3O_2$ $[M+H]^+$: 310.09863; Found: 310.10159.

*4.2.17. 2-Fluoro-4-((5-(4-fluorophenyl)-1,3,4-oxadiazol-2-yl) methoxy)benzonitrile **(7i)***

Yield: 81%; mp: 140–142 °C, white powder; IR (KBr) ν max: 3108, 2822, 2233, 1609, 1017, 855 cm^{-1}; ^1H NMR ($CDCl_3$, 400 MHz, ppm): δ 8.03–7.99 (m, 2H), 7.52–7.50 (m, 1H), 7.19–7.13 (m, 2H), 6.90–6.83 (m, 2H), 5.31 (s, 2H); ^{13}C NMR (100 MHz, $CDCl_3$, ppm): δ 165.4, 165.16 (d, *J* = 252 Hz), 164.4 (d, *J* = 258 Hz), 162.2, 162.1, 160.8, 134.72, 134.7, 129.6, 129.5, 119.5, 119.4, 116.7, 116.5, 113.8, 111.6, 111.5, 103.7, 103.5, 95.1, 94.9, 60.1; HRMS (ESI): *m/z* calculated for $C_{16}H_9F_2N_3O_2$ $[M+H]^+$: 314.07356; Found: 314.07275.

*4.2.18. 4-((5-(4-chlorophenyl)-1,3,4-oxadiazol-2-yl)methoxy)-2-fluorobenzonitrile **(7j)***

Yield: 90%; mp: 166–168 °C, white powder; IR (KBr) ν max: 3102, 2232, 1624, 1017, 839, 728 cm^{-1}; ^1H NMR ($CDCl_3$, 400 MHz, ppm): δ 7.94 (d, *J* = 8.8 Hz, 2H), 7.54–7.50 (m, 1H), 7.44 (d, *J* = 8.4 Hz, 2H), 7.19 (s, 1H), 6.90–6.83 (m, 1H), 5.31 (s, 2H); ^{13}C NMR (100 MHz, $CDCl_3$, ppm): δ 164.4, 163.4 (d, *J* = 258 Hz), 159.8, 137.7, 133.7, 133.6, 128.6, 127.4, 120.5, 112.8, 110.5, 110.4, 102.7, 102.5, 59.0; HRMS (ESI): *m/z* calculated for $C_{16}H_9ClFN_3O_2$ $[M+H]^+$: 330.04401; Found: 330.04364.

*4.2.19. 2-((4-(1,3,4-oxadiazol-2-yl)phenoxy)methyl)-5-phenyl-1,3,4-oxadiazole **(7k)***

Yield: 80%; mp: 154–156 °C; Appearance: white powder; IR (KBr) ν max: 3130, 1612, 836 cm^{-1}; ^1H NMR ($CDCl_3$, 400 MHz, ppm): δ 8.36 (s, 1H), 7.99 (s, 4H), 7.45 (d, *J* = 7.2 Hz, 3H), 7.12 (d, *J* = 8 Hz, 2H), 5.34 (s, 2H);^{13}C NMR ($CDCl_3$, 100 MHz, ppm): δ 166.0, 164.3, 161.6, 160.2, 152.4, 132.2, 129.2, 129.1, 127.1, 123.3, 117.5, 115.4, 59.9; HRMR (ESI): *m/z* calculated for $C_{17}H_{12}N_4O_3$ $[M+H]^+$: 321.09822; Found: 321.10147.

*4.2.20. 2-((4-(1,3,4-oxadiazol-2-yl)phenoxy)methyl)-5-(4-methoxyphenyl)-1,3,4-oxadiazole **(7l)***

Yield: 87%; mp: 150–152 °C; Appearance: white powder; IR (KBr) ν max: 3136, 2918, 1617, 845 cm^{-1}; ^1H NMR ($CDCl_3$, 400 MHz, ppm): δ 8.36 (s, 1H), 7.99–7.92 (m, 4H), 7.11 (d, *J* = 8.4 Hz, 2H), 6.93 (d, *J* = 8 Hz, 2H), 5.31 (s, 2H), 3.80 (s, 3H); ^{13}C NMR ($CDCl_3$, 100 MHz, ppm): δ 165.9, 164.3, 162.7, 161.1, 160.3, 152.3, 129.1, 128.9, 117.5, 115.8, 115.4, 114.5, 59.9, 55.4; HRMR (ESI): *m/z* calculated for $C_{18}H_{14}N_4O_4$ $[M+H]^+$: 351.10878; Found: 351.10818.

*4.2.21. 2-((4-(1,3,4-oxadiazol-2-yl)phenoxy)methyl)-5-(p-tolyl)-1,3,4-oxadiazole **(7m)***

Yield:85%; mp:170–172 °C; Appearance: white powder; IR (KBr) ν max: 3096, 2922, 2863, 1612, 816 cm^{-1}; ^1H NMR ($CDCl_3$, 400 MHz, ppm): δ 8.36 (s, 1H), 7.98 (d, *J* = 8.8 Hz, 2H), 7.88 (d, *J* = 8 Hz, 2H), 7.23 (d, *J* = 8 Hz, 2H), 7.11 (d, *J* = 8.4 Hz, 2H), 5.32 (s, 2H), 2.35 (s, 3H); ^{13}C NMR ($CDCl_3$, 100 MHz, ppm): δ166.2, 164.3, 161.3, 160.3, 152.3, 142.8, 129.8, 129.1, 127.1, 120.5, 117.5, 115.4, 59.9, 21.6; HRMR (ESI): *m/z* calculated for $C_{18}H_{14}N_4O_3$ $[M+H]^+$: 335.11387; Found: 335.11353.

*4.2.22. 2-((4-(1,3,4-oxadiazol-2-yl)phenoxy)methyl)-5-(4-fluorophenyl)-1,3,4-oxadiazole **(7n)***

Yield: 92%; mp:164–166 °C; Appearance: white powder; IR (KBr) ν max: 3100, 2920, 1612, 1036, 845 cm^{-1}; ^1H NMR ($CDCl_3$, 400 MHz, ppm): δ 8.37 (s, 1H), 8.02–7.98 (m, 4H), 7.14–7.10 (m, 4H), 5.34 (s, 2H); ^{13}C NMR ($CDCl_3$, 100 MHz, ppm): δ 165.2, 165.1 (d, *J* = 252 Hz), 164.3, 161.6, 160.2, 152.3, 129.5, 129.4, 129.1, 119.7, 119.6, 117.6, 116.6, 116.4, 115.3, 59.8; HRMR (ESI): *m/z* calculated for $C_{17}H_{11}FN_4O_3$ $[M+H]^+$: 339.08879; Found: 339.08829.

*4.2.23. 2-((4-(1,3,4-oxadiazol-2-yl)phenoxy)methyl)-5-(4-chlorophenyl)-1,3,4-oxadiazole **(7o)***

Yield: 89%; mp: 166–168 °C; Appearance: white powder. IR (KBr) ν max: 3110, 2920, 1611, 845 cm^{-1}.^1H NMR ($CDCl_3$, 400 MHz, ppm): δ 8.37 (s, 1H), 8.01–7.94 (m, 3H), 7.43 (d, *J* = 8.4 Hz, 2H), 7.19 (s, 1H), 7.12 (d, *J* = 8.8 Hz, 2H), 5.34 (s, 2H). ^{13}C NMR ($CDCl_3$, 100 MHz, ppm): δ 165.2, 164.3, 161.7, 160.2, 152.3, 138.6, 129.6, 129.1, 128.4, 121.7, 117.6, 115.3, 59.8. HRMR (ESI): *m/z* calculated for $C_{17}H_{11}ClN_4O_3$ $[M+H]^+$: 355.05924; Found: 355.05887.

4.3. Biological evaluation

4.3.1. Cytotoxicity assay

Breast cancer cell lines (MCF-7 & MDA-MB-453) and non-cancerous cell line (MCF-10A) were obtained from NCCS Pune. The cells were cultured using DMEM with 10% FBS. The cells were incubated at 37 °C with 5% CO_2. After achievement of 70–80% confluence, the cells were trypsinized and harvested. Approximately 5000 cells/well were seeded into a 96 well cell culture plate. The cells were incubated to recover from handling for 24 h. The Anti-cancer activity was measured by adding the test compounds of concentrations up to 100 μM. Test compounds dissolved in DMSO was added to each well and control wells contain DMSO without test compounds. Then the plate was incubated for 48 h to allow the test compound to take effect. The culture medium was changed at the end of the treatment, and 10 μL of MTT (5 mg/ml) was added to each well and incubated for an additional 4 h. The medium was aspirated, and formazan crystals were dissolved in 150 μL DMSO/well, and optical density was measured at 560 nm. For each concentration of test compounds, triplicates were performed, and the average value was considered.

4.3.2. Acridine orange (AO)/ethidium bromide (EtBr) dual staining

For conventional AO/EtBr apoptosis assay 5×10^5 cells/well

were seeded in a 6 well plate and incubated (37 °C and 5% CO_2) for overnight. MDA-MB 453 cell lines were treated with the test compound for 48 h. The concentration of dye was prepared as 1:1 ratio, each dye concentration was 100 μg/mL. Cells were stained with 8 μL of dye for 5 min, and images were taken immediately by fluorescence microscopy.

4.3.3. DNAMethyl transferase enzyme inhibitor assay

DNMT inhibition assay was carried out using EpiQuik DNA methyltransferase activity/inhibition screening assay kit (Epigentek, Brooklyn, NY, USA) according to the manufacturer's instruction.

4.3.4. PCR

MDA-MB 453 cells (1×10^6) were cultured in 100 mm Petri dishes. After attaining 70–80% confluence, the cells were incubated with different concentration of test drug for 48 h. Total RNA was isolated from the cells using TRI reagent (sigma life science) and quantified by quick drop (Molecular Devices). The total RNA was converted to cDNA using High capacity cDNA reverse transcription conversion kit (Applied Biosystems). Total RNA (3 μg) from each sample was subjected to reverse transcription according to the manufacturer protocol. The PCR products were resolved by electrophoresis through a 2% agarose gel and stained with ethidium bromide. The intensities of PCR product in the agarose gel were scanned with G: BOX (Syngene) image scanner.

Acknowledgements

This work was supported by Govt. of India funded by the Ministry of Science & Technology, Department of Biotechnology (DBT) (Sanctioned No. BT/PR16268/NER/95/183/2015).

Dr. R. Elancheran thank DST-PURSE phase II for the support as Research Associate. We would like to acknowledge Dr. Atanu Bhattacharjee, Department of Biotechnology & Bioinformatics, NEHU for his endless help during few experiments.

Appendix A. Supplementary data

Supplementary data to this article can be found online at https://doi.org/10.1016/j.ejmech.2019.02.033.

Conflicts of interest

The Authors declare no competing interests.

References

[1] A.M. Noone, D. Miller, A. Brest, M. Yu, J. Ruhl, Z. Tatalovich, A. Mariotto, et al., SEER cancer statistics review, 1975–2015, in: Based on November 2017 SEER Data Submission, Posted to the SEER Web Site, National Cancer Institute, Bethesda, MD, 2018. April 2018.
[2] J. Ferlay, I. Soerjomataram, M. Ervik, R. Dikshit, S. Eser, C. Mathers, M. Rebelo, D.M. Parkin, D. Forman, F. Bray, GLOBOCAN 2012 v1.0, Cancer Incidence and Mortality Worldwide: IARC Cancer Base No. 11, International Agency for Research on Cancer, Lyon, France, 2013, 2015.
[3] V.L. Maruthanila, R. Elancheran, A.B. Kunnumakkara, S. Kabilan, J. Kotoky, Recent development of targeted approaches for the treatment of breast cancer, Breast Canc. 24 (2017) 191–219.
[4] C.K. Osborne, Tamoxifen in the treatment of breast cancer, N. Engl. J. Med. 339 (1998) 1609–1618.
[5] C.Y. Liu, M.H. Hung, D.S. Wang, P.Y. Chu, J.C. Su, T.H. Teng, C.T. Huang, et al., Tamoxifen induces apoptosis through cancerous inhibitor of protein phosphatase 2A–dependent phospho-Akt inactivation in estrogen receptor–negative human breast cancer cells, Breast Cancer Res. 16 (2014) 431.
[6] S. Narrandes, S. Huang, L. Murphy, W. Xu, The exploration of contrasting pathways in triple negative breast cancer (TNBC), BMC Canc. 18 (2018) 22.
[7] I. Peralta-Arrieta, D. Hernández-Sotelo, Y. Castro-Coronel, M.A. Leyva-Vázquez, B. Illades-Aguiar, DNMT3B modulates the expression of cancer-related genes and downregulates the expression of the gene VAV3 via methylation, Am. J. Cancer Res. 7 (2017) 77–87.
[8] Z. Zhang, Y. Fan, F. Xie, H. Zhou, K. Jin, L. Shao, W. Shi, P. Fang, B. Yang, H. van Dam, P. ten Dijke, Breast cancer metastasis suppressor OTUD1 deubiquitinates SMAD7, Nat. Commun. 8 (2017) 2116, https://doi.org/10.1038/s41467-017-02029-7.
[9] P. Martins, J. Jesus, S. Santos, L. Raposo, C. Roma-Rodrigues, P. Baptista, A. Fernandes, Heterocyclic anticancer compounds: recent advances and the paradigm shift towards the use of nanomedicine's tool box, Molecules 20 (2015) 16852–16891.
[10] R. Elancheran, V.L. Maruthanila, M. Ramanathan, S. Kabilan, R. Devi, A. Kunnumakara, J. Kotoky, Recent discoveries and developments of androgen receptor based therapy for prostate cancer, Med. Chem. Comm. 6 (2015) 746–768.
[11] R. Gudipati, R.N. Anreddy, S. Manda, Synthesis, characterization and anticancer activity of certain 3-{4-(5-mercapto-1, 3, 4-oxadiazole-2-yl) phenylimino} indolin-2-one derivatives, Saudi Pharmaceut. J. 19 (2011) 153–158.
[12] X. Gan, D. Hu, Z. Chen, Y. Wang, B. Song, Synthesis and antiviral evaluation of novel 1, 3, 4-oxadiazole/thiadiazole-chalcone conjugates, Bioorg. Med. Chem. Lett 27 (2017) 4298–4301.
[13] R.A. Rane, S.D. Gutte, N.U. Sahu, Synthesis and evaluation of novel 1, 3, 4-oxadiazole derivatives of marine bromopyrrole alkaloids as antimicrobial agent, Bioorg. Med. Chem. Lett 22 (2012) 6429–6432.
[14] H. Rajak, A. Agarawal, P. Parmar, B.S. Thakur, R. Veerasamy, P.C. Sharma, M.D. Kharya, 2, 5-Disubstituted-1, 3, 4-oxadiazoles/thiadiazole as surface recognition moiety: design and synthesis of novel hydroxamic acid based histone deacetylase inhibitors, Bioorg. Med. Chem. Lett 21 (2011) 5735–5738.
[15] M.M. El-Din, M.I. El-Gamal, M.S. Abdel-Maksoud, K.H. Yoo, C.H. Oh, Synthesis and in vitro antiproliferative activity of new 1, 3, 4-oxadiazole derivatives possessing sulfonamide moiety, Eur. J. Med. Chem. 90 (2015) 45–52.
[16] M.M. El-Din, M.I. El-Gamal, M.S. Abdel-Maksoud, K.H. Yoo, C.H. Oh, Synthesis and broad-spectrum antiproliferative activity of diarylamides and diarylureas possessing 1, 3, 4-oxadiazole derivatives, Bioorg. Med. Chem. Lett 25 (2015) 1692–1699.
[17] V.R. Pidugu, N.S. Yarla, S.R. Pedada, A.M. Kalle, A.K. Satya, Design and synthesis of novel HDAC8 inhibitory 2, 5-disubstituted-1, 3, 4-oxadiazoles containing glycine and alanine hybrids with anti cancer activity, Bioorg. Med. Chem. 24 (2016) 5611–5617.
[18] A.V. Lee, S. Oesterreich, N.E. Davidson, MCF-7 cells-changing the course of breast cancer Research and care for 45 years, J. Natl. Cancer Inst. 107 (2015) 1–4, https://doi.org/10.1093/jnci/djv073.
[19] V.I. Balas, C.N. Banti, N. Kourkoumelis, S.K. Hadjikakou, G.D. Geromichalos, D. Sahpazidou, L. Male, M.B. Hursthouse, B. Bednarz, M. Kubicki, K. Charalabopoulos, Structural and in vitro biological studies of organotin (IV) precursors; selective inhibitory activity against human breast cancer cells, positive to estrogen receptors, Aust. J. Chem. 65 (2013) 1625–1637.
[20] G. Latsis, C. Banti, N. Kourkoumelis, C. Papatriantafyllopoulou, N. Panagiotou, A. Tasiopoulos, A. Douvalis, A. Kalampounias, T. Bakas, S. Hadjikakou, Poly organotin acetates against DNA with possible implementation on human breast cancer, Int. J. Mol. Sci. 19 (2018) 2055, https://doi.org/10.3390/ijms19072055.
[21] C.N. Banti, L. Kyros, G.D. Geromichalos, N. Kourkoumelis, M. Kubicki, S.K. Hadjikakou, A novel silver iodide metalo-drug; experimental and computational modeling assessment of its interaction with intracellular DNA, lipoxygenase and glutathione, Eur. J. Med. Chem. 77 (2014) 388–399.
[22] R.E. Hall, S.N. Birrell, W.D. Tilley, R.L. Sutherland, MDA-MB-453, an androgen-responsive human breast carcinoma cell line with high level androgen receptor expression, Eur. J. Cancer 30 (1994) 484–490.
[23] E.I. Gkaniatsou, C.N. Banti, N. Kourkoumelis, S. Skoulika, M. Manoli, A.J. Tasiopoulos, S.K. Hadjikakou, Novel mixed metal Ag(I)-Sb(III)-metallotherapeutics of the NSAIDs, aspirin and salicylic acid: enhancement of their solubility and bioactivity by using the surfactant CTAB, J. Inorg. Biochem. 150 (2015) 108–119.
[24] C.N. Banti, C. Papatriantafyllopoulou, M. Manoli, A.J. Tasiopoulos, S.K. Hadjikakou, Nimesulide silver metallodrugs, containing the mitochondriotropic, triaryl derivatives of pnictogen; anticancer activity against human breast cancer cells, Inorg. Chem. 55 (2016) 8681–8696.
[25] Schrödinger, LLC, New York, NY, 2013.
[26] A.K. Shiau, D. Barstad, P.M. Loria, L. Cheng, P.J. Kushner, D.A. Agard, G.L. Greene, The structural basis of estrogen receptor/coactivator recognition and the antagonism of this interaction by tamoxifen, Cell 95 (1998) 927–937.
[27] K.K. Jha, A. Samad, Y. Kumar, M. Shaharyar, R.L. Khosa, J. Jain, V. Kumar, P. Singh, Design, synthesis and biological evaluation of 1, 3, 4-oxadiazole derivatives, Eur. J. Med. Chem. 45 (2010) 4963–4967.
[28] H.S. Kareem, N. Nordin, T. Heidelberg, A. Abdul-Aziz, A. Ariffin, Conjugated oligo-aromatic compounds bearing a 3, 4, 5-trimethoxy moiety: investigation of their antioxidant activity correlated with a DFT study, Molecules 21 (2016) 224.
[29] G.M. Sheldrick, Acta Crystallogr. C71 (2015) 3.
[30] K. Lakshmithendral, K. Archana, K. Saravanan, S. Kabilan, S. Selvanayagam, Crystal structures of 3-methoxy-4-{[5-(4-methoxyphenyl)-1, 3, 4-oxadiazol-2-yl] methoxy} benzonitrile and N-(4-{[5-(4-chlorophenyl)-1, 3, 4-oxadiazol-2-yl] methoxy} phenyl) acetamide, Acta Crystallogr. E Crystallogr. Commun. 74 (2018) 1919–1922.
[31] S.A. Anand, C. Loganathan, N.S. Thomas, K. Saravanan, A.T. Alphonsa,

S. Kabilan, Synthesis, structure prediction, pharmacokinetic properties, molecular docking and antitumor activities of some novel thiazinone derivatives, New J. Chem. 39 (2015) 7120–7129.
[32] R. Elancheran, K. Saravanan, B. Choudhury, S. Divakar, S. Kabilan, M. Ramanathan, B. Das, R. Devi, J. Kotoky, Design and development of oxobenzimidazoles as novel androgen receptor antagonists, Med. Chem. Res. 25 (2016) 539–552.
[33] B. Choudhury, R. Kandimalla, R. Elancheran, R. Bharali, J. Kotoky, Garcinia morella fruit, a promising source of antioxidant and anti-inflammatory agents induces breast cancer cell death via triggering apoptotic pathway, Biomed. Pharmacother. 103 (2018) 562–573.
[34] S. Divakar, K. Saravanan, P. Karthikeyan, R. Elancheran, S. Kabilan, K.K. Balasubramanian, R. Devi, J. Kotoky, M. Ramanathan, Iminoenamine based novel androgen receptor antagonist exhibited anti-prostate cancer activity in androgen independent prostate cancer cells through inhibition of AKT pathway, Chem. Biol. Interact. 275 (2017) 22–34.
[35] K. Saravanan, R. Elancheran, S. Divakar, S. Athavan Alias Anand, M. Ramanathan, Jibon Kotoky, N.K. Lokanath, S. Kabilan, Design, synthesis and biological evaluation of 2-(4-phenylthiazol-2-yl) isoindoline-1, 3-dione derivatives as anti-prostate cancer agents, Bioorg. Med. Chem. Lett 27 (2017) 1199–1204.
[36] R. Elancheran, K. Saravanan, S. Divakar, S. Kumari, V.L. Maruthanila, S. Kabilan, M. Ramanathan, R. Devi, J. Kotoky, Design, Synthesis and biological evaluation of Novel 1, 3-thiazolidine-2, 4-diones as anti-prostate cancer agents, Anti Cancer Agents Med. Chem. 17 (2017) 1756–1768.
[37] M. Keimling, L. Wiesmüller, DNA double-strand break repair activities in mammary epithelial cells––influence of endogenous p53 variants, Carcinogenesis 30 (2009) 1260–1268.
[38] V.L. Maruthanila, R. Elancheran, N.K. Roy, A. Bhattacharya, A.B. Kunnumakkara, S. Kabilan, J. Kotoky, In silico molecular modelling of selected natural ligands and their binding features with estrogen receptor alpha, Curr. Comput. Aided Drug Des. (2018), https://doi.org/10.2174/1573409914666181008165356.